

Spyros D. Mentzelopoulos
Maria Theodoridou
Sotirios Malachias
Sotiris Sourlas
Demetrios N. Exarchos
Demetrios Chondros
Charis Roussos
Spyros G. Zakyntinos

Scanographic comparison of high frequency oscillation with versus without tracheal gas insufflation in acute respiratory distress syndrome

Received: 30 August 2010
Accepted: 14 December 2010
Published online: 3 March 2011
© Copyright jointly held by Springer and ESICM 2011

Electronic supplementary material

The online version of this article (doi:10.1007/s00134-011-2162-z) contains supplementary material, which is available to authorized users.

S. D. Mentzelopoulos (✉) ·
M. Theodoridou · S. Malachias · S. Sourlas ·
C. Roussos · S. G. Zakyntinos
First Department of Intensive Care
Medicine, Evangelismos General Hospital,
University of Athens Medical School,
45–47 Ipsilandou Street,
10675 Athens, Greece
e-mail: sdm@hol.gr;
sdmentzelopoulos@yahoo.com
Tel.: +30-6977-465832
Fax: +30-210-3218493

D. N. Exarchos · D. Chondros
Department of Radiology, Evangelismos
General Hospital, Athens, Greece

Abstract Purpose: In acute respiratory distress syndrome (ARDS), combined high frequency oscillation (HFO) and tracheal gas insufflation (TGI) improves oxygenation versus standard HFO, likely through TGI-induced lung recruitment. Experimental data suggest that steady flows such as TGI favor the filling of the lower (i.e., subcarinal) lung. We used whole-lung computerized tomography (CT) to determine whether HFO-TGI versus HFO improves the recruitment of the lower lung, and especially of its dependent region, where loss of aeration is maximized in ARDS. **Methods:** We enrolled 15 patients who had ARDS for 96 h or less, and pulmonary infiltrates in at least three chest X-ray quadrants. Patients were subjected to whole-lung CT after lung-protective conventional mechanical ventilation (CMV) and after 45 min of HFO and 45 min of HFO-TGI. HFO/HFO-TGI were employed in random order. CT scans were obtained at a continuous positive airways pressure equal to the mean tracheal pressure (P_{tr}) of CMV. During HFO/HFO-TGI, mean airway

pressure was titrated to the CMV P_{tr} level. Gas exchange and intra-arterial pressure/heart rate were determined for each ventilatory technique. **Results:** Regarding total lung parenchyma, HFO-TGI versus HFO and CMV resulted in a lower percentage of nonaerated lung tissue (mean \pm SD, $51.4 \pm 5.1\%$ vs. $60.0 \pm 2.5\%$, and $62.1 \pm 9.0\%$, respectively; $P \leq 0.04$); this was due to HFO-TGI-induced recruitment of nonaerated tissue in the dependent and nondependent lower lung. HFO-TGI increased normally aerated tissue versus CMV ($P = 0.04$) and poorly aerated tissue versus HFO and CMV ($P \leq 0.04$), and improved oxygenation versus HFO and CMV ($P \leq 0.04$). **Conclusions:** HFO-TGI improves oxygenation versus HFO and CMV through the recruitment of previously nonaerated lower lung units.

Keywords Respiratory distress syndrome · Adult · Respiration · Artificial · High frequency ventilation · Computed tomography

Introduction

In acute respiratory distress syndrome (ARDS), combined high frequency oscillation (HFO) and tracheal gas insufflation (TGI) improves gas exchange relative to HFO

without TGI at the same mean airway pressure (P_{aw}) [1, 2] and mean tracheal pressure (P_{tr}) [3]. Continuous, forward-thrust TGI exerts a positive end-expiratory pressure (PEEP) effect by impeding the opposite-directed expiratory flow [1–4]. Recent data, including esophageal

pressure measurements [3], suggest a TGI-related increase in lung volume, which largely explains the improvements in oxygenation and $PaCO_2$ when TGI is added to HFO. This implies a TGI-induced lung recruitment, partly achieved through its PEEP effect [3].

Steady flows, such as TGI, probably favor the filling of the lower lung, because the branching angles of the lower and right middle lobar and segmental bronchi are less acute compared to the branching angles of the upper lobar and segmental bronchi [5]. Consequently, the addition of TGI to HFO should mainly enhance the aeration of the lung parenchyma located below the carina [3, 5]. This potential effect should be more prominent in dependent, lower lung regions, in which the ARDS-related loss of aeration is maximized [6–9].

Preceding studies [1, 3] could not elucidate the effect of HFO-TGI on regional lung aeration. Besides recruitment, TGI could enhance the asymmetry between inspiratory and expiratory impedances observed during HFO [3, 10], and concurrently contribute to hyperinflation [1, 10]. Whole-lung computed tomography (CT) is the gold standard method of assessment of regional lung aeration [8, 9, 11–13]. In this study, we used CT to compare the regional effects of HFO and HFO-TGI at a pre-specified P_{tr} level. We theorized that HFO-TGI would mainly reduce the amount of nonaerated lung tissue, especially in the dependent, lower lung, and thus improve both overall and lower lung aeration.

Methods

Patients

Institutional approval and informed, written next-of-kin consent were obtained. Patients had ARDS [14] for 96 h or less. PaO_2 /inspired O_2 fraction (FiO_2) was within 80–199 mmHg with a PEEP of at least 8 cmH₂O for longer than 12 h. Pulmonary infiltrates were present in at least three frontal chest X-ray quadrants (Murray chest roentgenogram score at least 3 [15]). Full eligibility criteria are provided in Table E1 of the “Electronic supplementary material” (ESM).

On study-enrollment, patients were anesthetized, intubated (8.5- to 9.0-mm orotracheal or 8.0- to 9.0-mm tracheostomy tube [3]), and mechanically ventilated (Maquet Servo 300C or Servo-i ventilator) in a semirecumbent position (ESM). Electrocardiographic lead II, intra-arterial pressure, and peripheral oxygen saturation (SpO_2) were monitored continuously. Patients were on lung-protective, low-volume, plateau pressure-limited, conventional mechanical ventilation (CMV) employing pre-specified PEEP/ FiO_2 combinations [16; ESM]. Gas exchange targets were $PaO_2 = 60$ –80 mmHg, $SpO_2 = 90$ –95%, and arterial pH = 7.20–7.45.

Study design

Pre-transportation period

Details are provided in the ESM. Within 60–40 min before transportation to the CT suite, cisatracurium (0.15 mg/kg) was administered, a 2-catheter (i.e., a TGI catheter and a pressure-measuring catheter)-circuit adapter system was introduced [3], and a recruitment maneuver [continuous positive airway pressure (CPAP) of 40 cmH₂O for 30 s at FiO_2 1.0] was performed. CMV was resumed, patients were placed supine, and P_{tr} was determined and termed the study P_{tr} level. The P_{tr} level was within less than 1 cmH₂O of the concurrent, conventional ventilator-displayed P_{aw} [3], which was also recorded and termed the study CMV P_{aw} . Subsequently, arterial blood gases, respiratory compliance [17], and Murray score [14] were determined.

At 40 min pre-transportation, patients were connected to the SensorMedics 3100B high frequency ventilator. Ventilator settings were $FiO_2 = 1.0$, bias flow = 60 L/min, frequency = 4.0 Hz, oscillatory pressure amplitude (ΔP) = 90 cmH₂O, and inspiratory-to-expiratory time ratio 1:2. Following HFO initiation, a reproducible [1, 3] cuff leak of 4–5 cmH₂O (corresponding to cuff deflation by 2.0–3.0 mL) was established, and the high frequency ventilator P_{aw} was titrated to the study P_{tr} level and its value recorded and termed the study HFO P_{aw} . Subsequently, continuous, forward-thrust TGI ($FiO_2 = 1.0$; flow = 50% of immediately preceding CMV minute ventilation) was added to HFO, and the high frequency ventilator P_{aw} was re-titrated to the study P_{tr} level and its value recorded and termed the study HFO-TGI P_{aw} .

At 20 min pre-transportation, the catheters were withdrawn and CMV was resumed. Following arrival at the CT suite, patients were placed supine on the CT scanner bed and reconnected to the intensive care unit (ICU) ventilator. CMV was continued at $FiO_2 = 1.0$ and all other original ICU settings were maintained unchanged. Subsequently, cisatracurium was re-administered.

Main study period

Figure 1 illustrates the main investigational interventions. A recruitment maneuver (CPAP = 40 cmH₂O for 30 s) was performed and the TGI catheter and pressure-measuring catheter were reintroduced through their respective adapters. The TGI catheter was proximally connected to a variable orifice O_2 flowmeter, with O_2 flow set at 0 L/min, whereas the proximal orifice of the pressure-measuring catheter was capped. We inserted both catheters to reproduce the pre-transportation, supine ventilatory conditions. This consistently resulted in a ventilator-displayed P_{aw} that was within less than 0.5 cmH₂O of the predetermined study CMV P_{aw} . Following 15 min of

equilibration, a set of physiological measurements (i.e., arterial/central-venous blood gas analyses, intra-arterial pressure and heart rate, and respiratory mechanics [17]) was obtained. Immediately after the end-inspiratory occlusion, the ICU ventilator was set at CPAP = predetermined study P_{tr} level and a whole-lung CT was performed (Fig. 1). Subsequently, patients were connected to the high frequency ventilator, the recruitment maneuver was repeated, and HFO or HFO-TGI (each for 45 min in random order) was initiated with the aforementioned pre-transportation, high frequency ventilator and/or TGI settings (including the predetermined study HFO P_{aw} or study HFO-TGI P_{aw}), and the same cuff leak. After every 45 min of HFO or HFO-TGI, blood gases and hemodynamics were redetermined and the whole-lung CT scan was repeated at high frequency ventilator-applied CPAP = study P_{tr} level (Fig. 1). Subsequently, patients were transported back to the ICU (ESM).

CT imaging and analysis

Helical CT scanning was performed on a Toshiba Aquilion 16-row detector CT scanner (detector configuration,

16×2.0 mm; z -direction length, 32 mm), software version V1.41ER001 (Toshiba, London, UK). CT scanner settings were contiguous slice thickness = 7 mm (voxel volume, ~ 4.2 mm³); speed, 30 mm/rotation; beam pitch, 0.9375 [18, 19]; exposure time = 0.50 s; voltage = 135 kV; and current = 200 mA. CT data analysis is detailed in the ESM. Briefly, in each CT section, the outline of the lungs was manually drawn (Fig. 1) by two investigators blinded to the employed ventilatory technique. Lung regions were classified as hyperinflated [CT number = -901 to $1,000$ Hounsfield units (HU)], normally aerated (CT number = -501 to 900 HU), poorly aerated (CT number = -101 to 500 HU), and nonaerated (CT number = $+100$ to 100 HU). Whole-lung results were expressed according to the varying degrees of aeration and corresponding percentage of lung tissue weight [13].

CT analysis was repeated after lung parenchymal subdivision in nondependent and dependent upper, and nondependent and dependent lower regions. Anterior (nondependent) and posterior (dependent) subdivision of CT sections is illustrated in Fig. 1. Lower lung ranged from the first subcarinal CT section to the last basal section. Upper lung extended from the CT section corresponding to the carina to the first apical section.

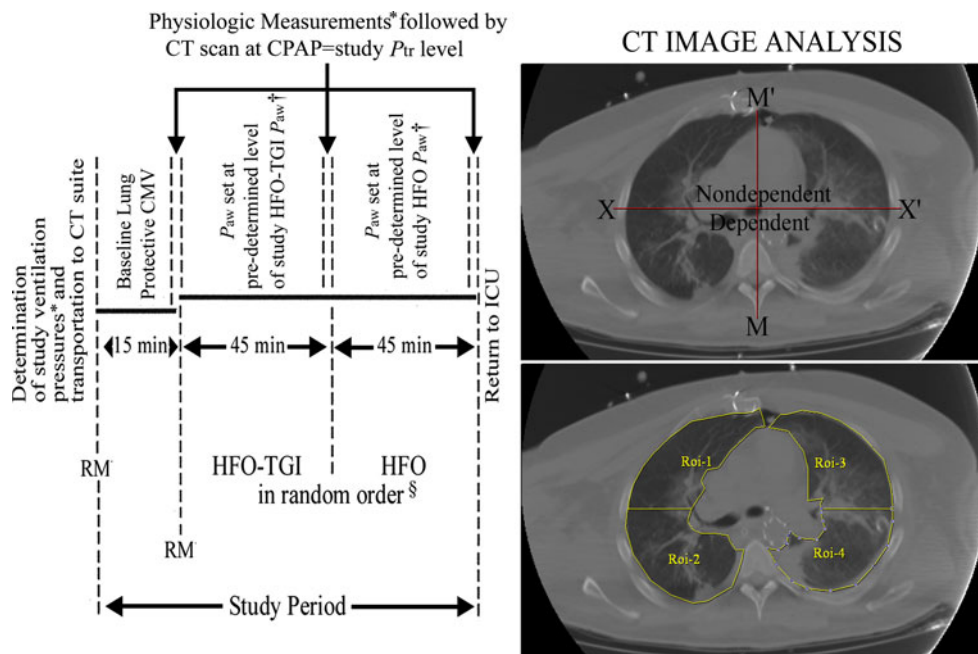


Fig. 1 Schematic representation of study methodology. CT computed tomography, RM recruitment maneuver, CMV conventional mechanical ventilation, HFO high frequency oscillation, TGI tracheal gas insufflation, P_{aw} mean airway pressure, P_{tr} mean tracheal pressure, CPAP continuous positive airways pressure, Roi region of interest. Left panel schematic representation of the investigational interventions of the study protocol; *see text for details; † P_{aw} settings were aimed at achieving the study P_{tr} level (see also “Methods”); §HFO preceded HFO-TGI in eight patients,

and the reverse order was followed in another seven patients; we did not perform any RM in-between HFO and HFO-TGI. Right upper panel in each CT section, the subdivision of lung parenchyma in anterior (nondependent) and posterior (dependent) regions was performed by drawing a line (XX') passing through the midpoint of and being vertical to the anteroposterior axis of the thoracic cavity (MM'). Right lower panel for each CT section, the aforementioned subdivision resulted in two nondependent Rois (i.e., Roi-1 and Roi-3) and two dependent Rois (i.e., Roi-2 and Roi-4)

Statistical analysis

According to an a priori power analysis, 15 patients were required for $\alpha = 0.04$, and power = 0.88 (see ESM). Data were analyzed with SPSS version 12.0 (SPSS, Chicago, IL, USA). The distribution normality was tested by the Kolmogorov–Smirnov test. For each ventilatory technique level, physiological and CT image analysis data were compared with repeated-measures analysis of variance for one within-subjects factor (i.e., ventilatory technique), followed by the Tukey test. Bivariate, least-squares, linear regression was used to interpret changes in physiological variables. Significance was accepted at $P < 0.05$. Data are reported as mean \pm SD.

Results

We enrolled 15 nonconsecutive patients with ARDS over a 3.5-year period (i.e., within 2006–2009). Table 1 displays the patients' baseline characteristics. There were no study protocol-related complications or instances of patient spontaneous breathing or coughing. SpO₂ was always at least 90% throughout study period.

Relative to baseline, the first set of study physiological measurements (Fig. 1) showed that transportation did not notably affect gas exchange (Tables 1, 2; ESM), inspiratory/expiratory CMV pressures, CMV P_{aw} (see also above and ESM), and respiratory resistance or compliance (ESM). Tracheal tube dimensions, insertion depth, and patency remained unchanged throughout the study (ESM). Thus, the pre-transportation, supine, CMV P_{tr} level (i.e., the study P_{tr} level) should have been re-achieved during pre-HFO/HFO-TGI CMV in the CT suite [3] (ESM). Also, in the presence of identical HFO/HFO-TGI settings (including bias flow and ΔP) and cuff leak, and unchanged tracheal tube characteristics, the use of study HFO/HFO-TGI P_{aw} in the CT suite should have reproduced the study P_{tr} level [3] (ESM).

The study HFO P_{aw} and HFO-TGI P_{aw} were 28.7 ± 1.5 and 27.4 ± 1.4 cmH₂O, respectively, and employed TGI flow was 6.1 ± 0.5 L/min (range 4.5–6.5); in the presence of a 4–5 cmH₂O cuff leak, the between- P_{aw} difference of 1.3 ± 0.3 cmH₂O reflected the TGI-induced increment in P_{tr} [3].

Whole-lung CT scans were performed at CPAP = 21.6 ± 1.7 cmH₂O (range 19.0–25.6) (study P_{tr} level; see also above and Table 1).

Physiological variables

Table 2 displays the gas exchange and hemodynamics results. HFO-TGI resulted in a higher PaO₂/FiO₂ and lower shunt fraction versus CMV and HFO ($P \leq 0.04$).

Table 1 Patient characteristics and baseline ventilatory settings (volume assist-control mode with square wave inspiratory flow)

Age (years)	54.3 \pm 20.4
Sex (male/female)	12:3
Body mass index (kg/m ²)	25.0 \pm 2.9
Simplified acute physiology II score ^a	37.5 \pm 12.6
Murray score ^b	3.4 \pm 0.3
PaO ₂ /inspired O ₂ fraction (mmHg) ^b	97.2 \pm 21.7
Inspired O ₂ fraction ^b	0.79 \pm 0.09
PaCO ₂ (mmHg) ^b	60.0 \pm 7.6
Arterial pH ^b	7.29 \pm 0.06
Positive end-expiratory pressure (cmH ₂ O) ^b	13.6 \pm 1.9
Tidal volume (L)/(mL/kg PBW) ^b	0.47 \pm 0.06/ 6.5 \pm 0.4
Respiratory rate (breaths/min) ^b	26.4 \pm 2.1
Minute ventilation (L/min) ^b	12.3 \pm 1.0
Inspiratory-to-expiratory time ratio ^{b,c}	1:2
End-inspiratory plateau airway pressure (cmH ₂ O) ^b	30.4 \pm 3.5
Mean airway pressure (cmH ₂ O) ^b	21.2 \pm 1.7
Mean tracheal pressure (cmH ₂ O) ^b	21.6 \pm 1.7
Oxygenation index ^b	22.5 \pm 4.1
Quasistatic respiratory compliance (mL/cmH ₂ O) ^{b,d}	32.0 \pm 7.0
Time from ARDS diagnosis (h) ^e	53.7 \pm 15.2
Pulmonary ARDS—no./total no. (%)	12/15 (80.0)
Survival to hospital discharge—no./total no. (%)	7/15 (46.7)

Values are mean \pm SD, unless otherwise specified. For males, PBW was calculated as $50 + [\text{height (cm)} - 152.4] \times 0.91$; for females, 50 was replaced by 45.5

PBW predicted body weight, ARDS acute respiratory distress syndrome

^a Determined within 12 h prior to study enrollment

^b Recorded/determined within 5–20 min after study enrollment

^c The protocol pre-specified value of 1:2 was pre-selected by the attending physicians in all patients

^d Determined as tidal volume (in mL) divided by the difference between end-inspiratory and end-expiratory plateau airway pressure

^e Refers to the time interval between the establishment of ARDS diagnosis and study enrollment

The arterial and central-venous PCO₂ and pH were improved during HFO-TGI versus CMV ($P \leq 0.03$). The oxygenation index was lower during HFO-TGI versus HFO ($P = 0.001$). The mean arterial pressure, heart rate, and central-venous O₂ saturation were unaffected by the ventilatory technique.

CT image analysis

The results are presented in Table 3. Regarding total lung parenchyma, HFO-TGI versus CMV resulted in higher lung volume ($P = 0.005$) and gas volume ($P = 0.002$). HFO-TGI versus HFO resulted in trends toward higher lung and gas volume ($P = 0.09$ – 0.10). The percentage of normally aerated lung parenchyma was higher during HFO-TGI versus CMV ($P = 0.04$). The percentage of poorly aerated parenchyma was higher during HFO-TGI versus CMV and HFO ($P \leq 0.04$), whereas percentage of

Table 2 Gas exchange and hemodynamic data of the main study period

Ventilatory strategy	PaO_2/FiO_2 (mmHg)	$PaCO_2$ (mmHg)	pHa	ScvO ₂ (%)	$PcvCO_2$ (mmHg)
CMV	90.1 ± 28.0	59.8 ± 7.9	7.28 ± 0.06	75.4 ± 4.1	64.9 ± 7.7
HFO	103.5 ± 28.3	56.1 ± 9.9	7.31 ± 0.06	75.9 ± 4.1	61.5 ± 9.5
HFO-TGI	139.2 ± 31.1 ^{*†}	50.8 ± 10.4 [*]	7.35 ± 0.07 [*]	73.7 ± 4.9	55.8 ± 10.4 [*]
Ventilatory strategy	pHcv	Shunt fraction	Oxygenation index	MAP (mmHg)	Heart rate (beats/min)
CMV	7.23 ± 0.06	0.43 ± 0.06	25.0 ± 5.5	90.2 ± 12.8	107.1 ± 12.0
HFO	7.26 ± 0.06	0.42 ± 0.08	29.8 ± 8.5	90.7 ± 13.3	108.3 ± 14.1
HFO-TGI	7.31 ± 0.08 [*]	0.35 ± 0.05 ^{*†}	20.8 ± 4.5 [†]	86.7 ± 12.4	104.3 ± 13.3

Values are mean ± SD. For the computation of shunt fraction, we used venous partial pressure, $pHcv$ central venous pH, MAP mean arterial pressure blood-gas values obtained from the central-venous blood [3, 13]

CMV conventional mechanical ventilation, HFO high frequency oscillation, * $P \leq 0.03$ versus CMV

TGI tracheal gas insufflation, Pa arterial partial pressure, FiO_2 inspired O₂ fraction, pHa arterial pH, $ScvO_2$ central-venous O₂ saturation, Pcv central

† $P \leq 0.04$ versus HFO

Table 3 Results of computed tomographic image analysis

Ventilatory strategy	Gas and tissue volume (mL)	Gas volume (mL)	Tissue weight (g)	Hyperinflated (tissue weight %)	Normally aerated (tissue weight %)	Poorly aerated (tissue weight %)	Nonaerated (tissue weight %)
Total lung parenchyma							
CMV	2,684.4 ± 272.5	786.5 ± 290.7	1,898.0 ± 177.4	0.01 ± 0.01	12.7 ± 6.5	24.8 ± 5.6	62.1 ± 9.0
HFO	2,780.6 ± 203.0	913.2 ± 199.4	1,867.4 ± 170.0	0.01 ± 0.01	15.3 ± 5.0	25.2 ± 7.3	60.0 ± 2.5
HFO-TGI	2,995.6 ± 181.5 [*]	1,087.1 ± 178.9 [*]	1,869.2 ± 192.6	0.01 ± 0.01	18.0 ± 5.3 [*]	30.7 ± 4.9 ^{*†}	51.4 ± 5.1 ^{*†}
Upper dependent							
CMV	197.0 ± 58.1	97.9 ± 38.2	99.2 ± 24.6	0.00 ± 0.00	35.7 ± 13.2	46.3 ± 9.4	18.0 ± 9.0
HFO	266.7 ± 38.2 [*]	131.7 ± 27.4 [*]	135.0 ± 24.7 [*]	0.00 ± 0.00	37.8 ± 13.9	49.2 ± 11.7	13.1 ± 4.8
HFO-TGI	261.2 ± 28.9 [*]	136.9 ± 22.9 [*]	124.3 ± 16.7 [*]	0.00 ± 0.00	44.5 ± 11.0	41.8 ± 7.9	13.7 ± 4.1
Lower dependent							
CMV	1,466.8 ± 168.3	161.2 ± 43.4	1,305.6 ± 192.7	0.00 ± 0.00	3.4 ± 2.0	20.4 ± 6.5	76.2 ± 7.0
HFO	1,379.0 ± 135.1	163.2 ± 19.5	1,215.9 ± 136.1	0.00 ± 0.00	4.1 ± 1.6	18.0 ± 4.1	78.0 ± 2.8
HFO-TGI	1,396.9 ± 162.4	225.1 ± 18.8 ^{*†}	1,171.8 ± 165.8	0.00 ± 0.00	5.6 ± 1.9 [*]	27.1 ± 3.6 ^{*†}	67.3 ± 3.0 ^{*†}
Upper nondependent							
CMV	281.0 ± 94.2	177.0 ± 73.3	104.0 ± 24.9	0.03 ± 0.04	49.1 ± 13.6	35.1 ± 9.5	15.8 ± 8.2
HFO	366.5 ± 68.6 [*]	227.7 ± 62.6	138.8 ± 17.3 [*]	0.02 ± 0.02	49.8 ± 15.2	38.6 ± 12.4	11.5 ± 4.6
HFO-TGI	370.0 ± 60.0 [*]	238.8 ± 53.6 [*]	131.9 ± 12.3 [*]	0.02 ± 0.02	56.8 ± 11.9	31.5 ± 8.4	11.7 ± 4.1
Lower nondependent							
CMV	730.5 ± 169.5	348.8 ± 142.9	381.8 ± 39.4	0.04 ± 0.05	26.2 ± 11.1	32.6 ± 9.2	41.2 ± 11.3
HFO	784.9 ± 139.9	408.0 ± 127.4	376.9 ± 26.4	0.05 ± 0.05	32.7 ± 10.5	28.5 ± 8.4	38.8 ± 3.1
HFO-TGI	951.9 ± 121.8 ^{*†}	513.6 ± 116.8 [*]	438.3 ± 25.7 ^{*†}	0.05 ± 0.04	35.0 ± 8.7	37.3 ± 6.7	27.7 ± 3.5 ^{*†}

Values are mean ± SD. Marginally non-significant differences, i.e., trends toward statistical significance corresponding to P values within 0.05–0.10, are detailed in the “Results”

CMV conventional mechanical ventilation, HFO high frequency oscillation, TGI tracheal gas insufflation

* $P \leq 0.04$ versus CMV

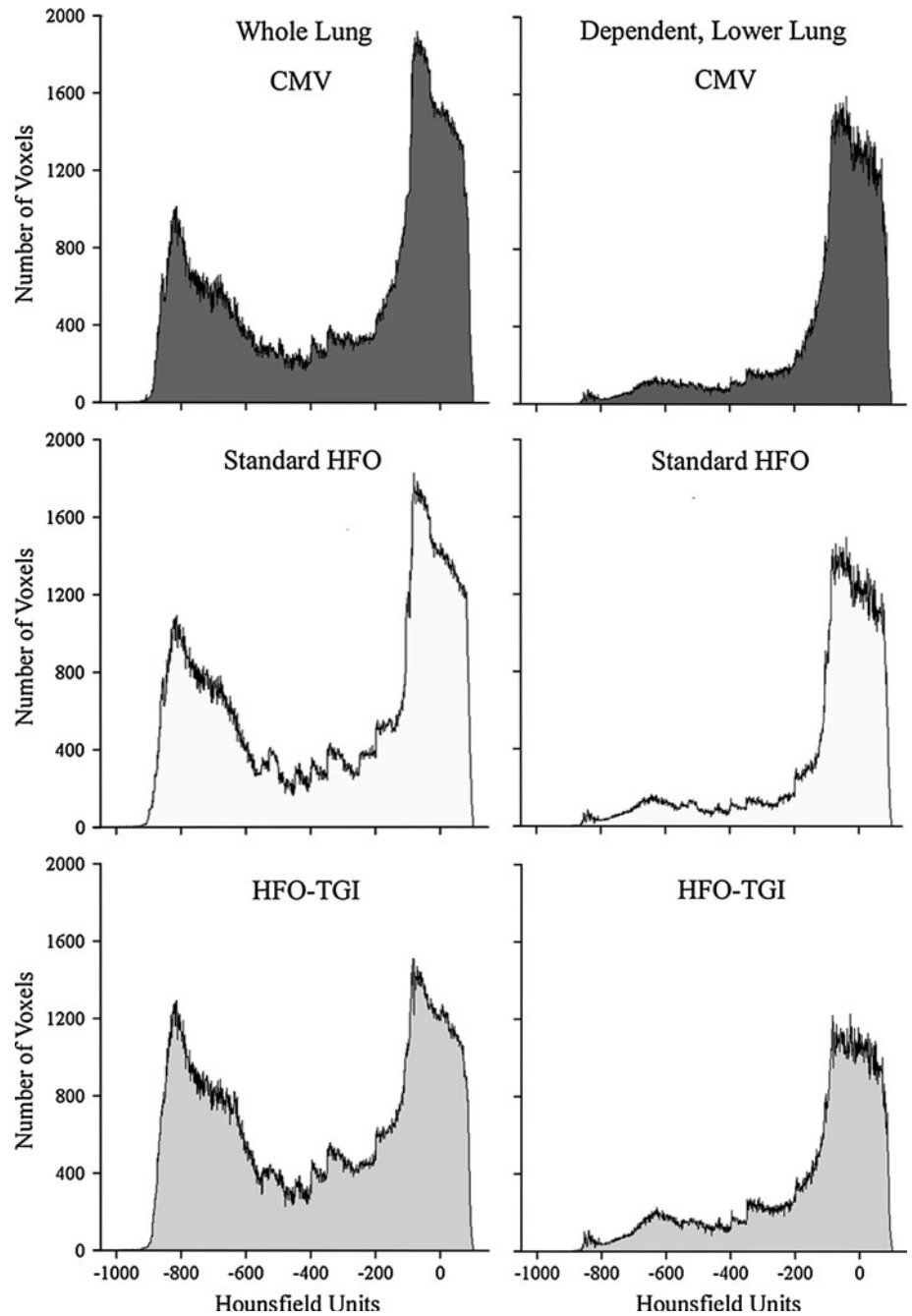
† $P \leq 0.04$ versus HFO

nonaerated parenchyma was lower during HFO-TGI versus CMV and HFO ($P \leq 0.001$). Notably, in the dependent, lower lung, we observed the same HFO-TGI-related improvements in the percentages of normally aerated (increased vs. CMV, $P = 0.005$), poorly aerated (increased vs. CMV and HFO, $P \leq 0.002$), and nonaerated (decreased vs. CMV and HFO, $P < 0.001$) parenchyma. Accordingly, the corresponding, regional gas volume was higher during HFO-TGI versus CMV and HFO ($P < 0.001$). Furthermore, in the nondependent, lower lung, there was an HFO-TGI-related decrease in the

percentage of nonaerated parenchyma versus CMV and HFO ($P < 0.001$). The corresponding regional lung volume and tissue weight were higher during HFO-TGI vs. CMV and HFO ($P \leq 0.009$); HFO-TGI resulted in a higher gas volume versus CMV ($P = 0.003$), and a trend toward higher gas volume versus HFO ($P = 0.08$). Figure 2 displays average density histograms for the whole lung and dependent, lower lung. Figure 3 displays lower lung CT sections from representative patients.

In the dependent and nondependent upper lung, ventilatory technique had no significant effect on the

Fig. 2 Average density histograms according to ventilatory technique. *CMV* conventional mechanical ventilation, *HFO* high frequency oscillation, *TGI* tracheal gas insufflation. *Left panel* whole-lung histograms. *Right panel* dependent, lower lung histograms. Voxel volume 4.2 mm³

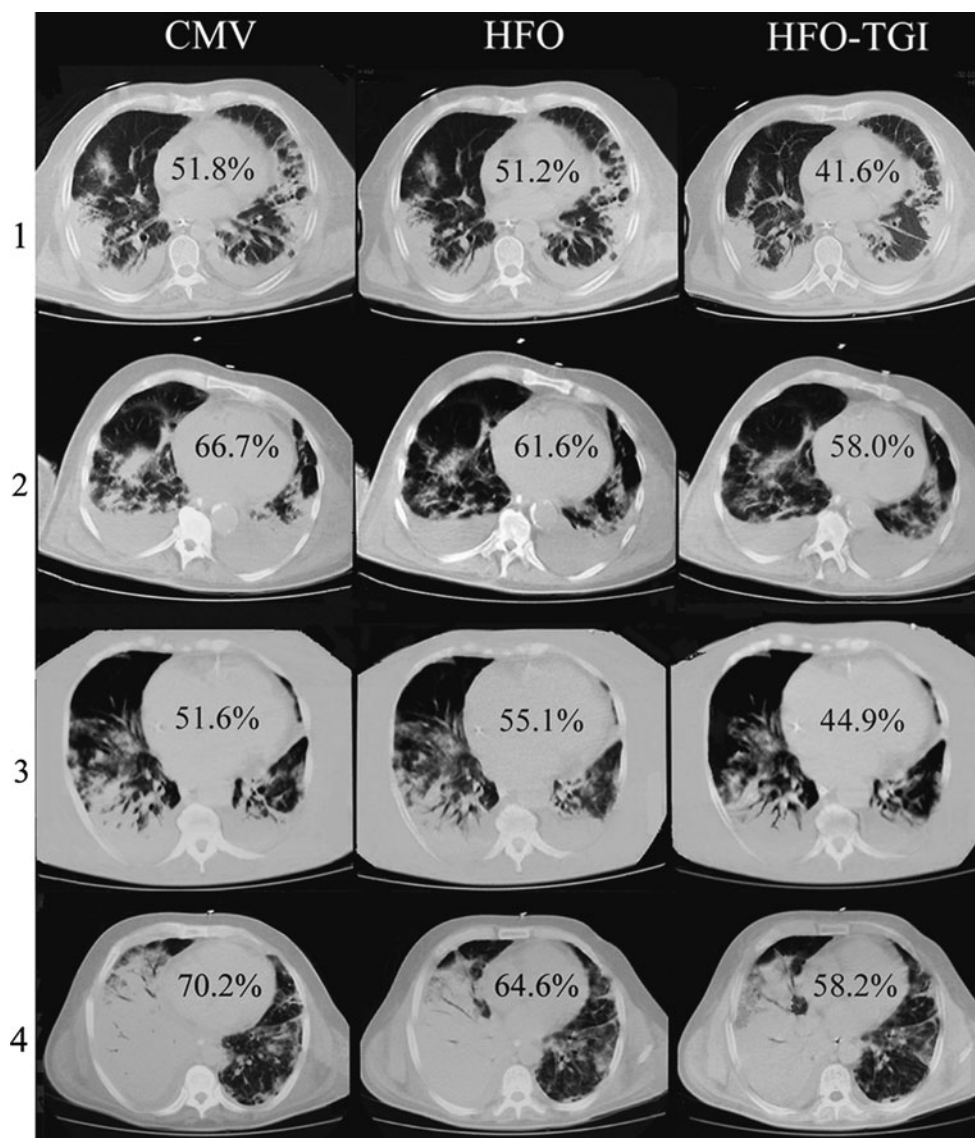


distribution of parenchymal aeration. However, both HFO and HFO-TGI were associated with increases in regional lung volume (average increase = 39.5–44.9%) and tissue weight (average increase = 31.2–41.8%) relative to CMV ($P \leq 0.01$). The average gas-to-tissue ratios of the HFO/HFO-TGI-induced lung volume increments ranged within 0.9–1.5 and 1.5–2.2 in the dependent and nondependent upper lung, respectively. There was no appreciable, HFO/HFO-TGI-related change in the percentage of hyperinflated lung tissue (Table 3).

Regression analysis

Changes in PaO_2/FiO_2 from CMV to HFO-TGI and from HFO to HFO-TGI were strongly correlated with concurrent changes in nonaerated, dependent, lower lung parenchyma ($R^2 = 0.61$ – 0.74 , $P \leq 0.001$; Fig. E5 of ESM). PaO_2/FiO_2 changes were also significantly correlated with concurrent changes in nonaerated, total lung parenchyma ($R^2 = 0.42$ – 0.43 , $P \leq 0.008$). Weaker correlations were observed between changes in shunt fraction

Fig. 3 Computed tomography (CT) sections of the lower lung from four representative patients (1–4). *CMV* conventional mechanical ventilation, *HFO* high frequency oscillation, *TGI* tracheal gas insufflation CT sections correspond to ~7 cm below the carina. In patients 1 and 3 HFO preceded HFO-TGI. In patients 2 and 4 HFO-TGI preceded HFO. Percentages reflect proportions of nonaerated lung tissue weight



and nonaerated, dependent, lower lung parenchyma ($R^2 = 0.30\text{--}0.33$, $P \leq 0.03$).

Discussion

HFO-TGI versus HFO and CMV resulted in a reduced amount of nonaerated lung tissue below the carina. During HFO-TGI, poorly aerated tissue increased versus HFO and CMV, and normally aerated tissue increased versus CMV. There were concurrent, HFO-TGI-related improvements in oxygenation and shunt fraction versus HFO and CMV, and $PaCO_2$ versus CMV. These results indicate improved lung recruitment and function with HFO-TGI.

In supine ARDS patients, loss of aeration predominates in dependent, lower lung regions, because it increases along both the anteroposterior and cephalocaudal axes [6–9]. Proposed mechanisms include reductions in regional transpulmonary pressure due to external compression by the heart [7, 8], pleural fluid collections [8], and abdominal contents [6, 8], and increased superimposed pressure exerted by the overlying, edematous lung tissue [9, 20, 21]. In these regions, “inflammatory” atelectasis (i.e., loss of gas volume with excess tissue volume/weight) and/or “compression” atelectasis (i.e., loss of gas volume without excess tissue volume/weight) predominate, and threshold opening pressures may range from ~15 to more than 30 cmH_2O [6, 21, 22].

In this study, most patients had moderate to severe hypoxemia during CMV, primary ARDS, and Murray

roentgenogram scores were at least 3 (Table 1). Accordingly, CT scanning revealed either diffuse or patchy attenuations [23]. These characteristics are consistent with increased recruitment potential, irrespective of ARDS etiology [13, 22]. Preceding experimental and clinical studies indicate that HFO exhibits time-dependent recruiting effects [24, 25]. This is partly attributable to minimal, distal, parenchymal, distending pressure swings during the respiratory cycle [24, 26], which should attenuate or prevent expiratory derecruitment [24]. Clinical HFO effects on oxygenation depend on the P_{aw}/P_{tr} level, and become evident after 1 h or longer (when HFO is combined with recruitment maneuvers [1, 3, 27, 28]) or 8 h or longer (when HFO is used alone [11, 23]).

Recently [3], 60-min sessions of HFO with P_{aw} titrated to the preceding CMV P_{tr} level did not improve oxygenation versus CMV. In contrast, 60-min sessions of HFO-TGI with P_{aw} titrated to the same P_{tr} level resulted in higher PaO_2/FiO_2 vs. both CMV and HFO. These results were largely attributed to a TGI-related PEEP effect and associated lung recruitment. Accordingly, in the present study, HFO did not significantly affect whole-lung aeration or gas exchange. In contrast, and in concordance with our hypothesis, HFO-TGI increased total lung and gas volume, largely by promoting penetration of gas into nonaerated, lower lung tissue, thus changing it into poorly aerated tissue participating in gas exchange (Table 3). This partly explains the observed reduction in pulmonary shunt (Table 2) at the employed FiO_2 of 1.0 [12].

Hypoxic pulmonary vasoconstriction is frequently impaired in ARDS [8]. Thus, the partial re-aeration of potentially well-perfused (due to gravitational effects) but previously nonaerated, dependent, lower lung regions should be a major cause of HFO-TGI-related oxygenation improvement. Accordingly, regression results showed that the reduction in nonaerated, dependent, lower lung tissue accounted for 61–74% of the TGI-induced oxygenation improvement (Table 2; Fig. E5 of ESM).

HFO and HFO-TGI had similar effects on upper lung aeration. This further confirms our hypothesis that TGI should primarily affect the lower lung. In the upper lung, the HFO/HFO-TGI-induced, concurrent increase in volume and tissue weight can be explained by a potential, early reopening of partially/totally collapsed small airways/alveoli. In cephalic lung regions, external compressive forces are absent and opening pressures of collapsed tissue are relatively low [6, 8, 9]. Also, our results did not reveal any concurrent, regional overdistention (Table 3). Thus, an earlier upper lung recruitment may have reduced regional pulmonary vascular resistance, with consequent blood flow diversion from still non-recruited lower lung units toward recruited upper lung units [12]. This in turn could have increased regional, extravascular lung water, because of the impaired microvascular permeability [29]. In the lower lung, the

same mechanism (i.e., earlier recruitment of nondependent/non-compressed vs. dependent/externally compressed lung units [6, 8, 9], causing blood flow diversion toward faster-recruited units) can explain the observed HFO-TGI-related increase in nondependent tissue weight (Table 3). This potential, dependent-to-nondependent blood flow shift is consistent with the HFO-TGI-related reduction in shunt fraction.

Methodological considerations

The lack of P_{tr} determination in the CT suite constitutes a limitation. However, such measurements would have necessitated the co-transport and recalibration of the pressure-measuring equipment (ESM), with a consequent increase in protocol duration/workload and associated safety issues. Furthermore, the unchanged CMV pressures, and ventilatory settings/conditions in the CT suite indicate that the study P_{tr} level was maintained throughout main study period (see “Results” and ESM).

We obtained the CT scans at CPAP level = study P_{tr} level in an effort to approximate the “average” ventilatory conditions during the use of different ventilatory techniques. This may have caused a minor underestimation of lung volume during HFO/HFO-TGI [24]. The periods of HFO/HFO-TGI use were short, and some time-dependent recruiting effects were likely missed. Another limitation was the lack of evaluation of regional lung perfusion [9].

HFO was used first in eight patients (Fig. 1), and relative to CMV, the HFO-recruited lung volume was 0.04 ± 0.10 L before HFO-TGI initiation (ESM). In the remaining seven patients, HFO-TGI was used first, and HFO-TGI-recruited volume was 0.33 ± 0.19 L before HFO initiation (ESM). The higher recruited volume of the “HFO-TGI-first subgroup” may have favorably affected our results on HFO.

Increasing the CT slice thickness and voxel volume may affect the accuracy of hyperinflation assessment [30, 31]. A voxel with CT attenuation greater than -900 HU may contain hyperinflated alveoli in a proportion insufficient to reduce its radiological density to less than -900 HU [22]. Our patients had diffuse aeration loss (Table 3), and the selection of 7-mm slice thickness instead of the 5-mm standard [13] had probably minor to negligible effects on our pulmonary subvolume measurements [30, 31].

Several prior studies have used at least two whole-lung CTs to evaluate the effect of PEEP on lung aeration [6, 12, 13, 22, 23, 30, 32, 33]. Also, several experts support the routine use of CT in ARDS management [8, 9, 34]. We used three whole-lung CTs to determine the effects of HFO and HFO-TGI on lung aeration. Following inspection of CT films, attending physicians of 12 study participants requested long-term HFO-TGI [35] for their patients.

Clinical implications

Our results indicate that when added to HFO, TGI improves oxygenation through a PEEP effect confined to the lower lung. We did not detect any concurrent, TGI-related, regional hyperinflation. We could not determine the degree of TGI flow penetration into lower-lung airways [3]. However, the high TGI jet stream velocity implies a short deadspace transit time and contribution to direct alveolar ventilation [3, 36]. Furthermore, as continuous, forward-thrust TGI opposes expiratory flow [1–4], its regional PEEP effect should comprise a regional increase in expiratory resistance and alveolar pressure. Such a selective, lower-lung recruiting effect may not be achievable through an increase in P_{aw} of HFO without TGI.

$PaCO_2$ results are consistent with a TGI-associated, improved deadspace clearance and augmentation of HFO tidal volume and alveolar ventilation [3]. HFO-TGI caused absolute reductions of ~9–11% in regional/overall nonaerated lung tissue and moderate gas exchange improvements. These effects may prove useful in patients

with severe oxygenation disturbances (e.g., PaO_2/FiO_2 less than 100 mmHg) and/or poor tolerance to hypercapnia [3, 35].

The limitations of long-term TGI include the absence of commercially available equipment, and possible tracheal mucosal damage, retention/inspissation of secretions, hemodynamic compromise, pneumothorax, and gas embolism [1, 3, 4]. For long-term HFO-TGI, we establish a cuff leak, and employ a single catheter-adaptor system for humidified TGI gas administration [3, 35].

Conclusions

HFO-TGI improves oxygenation versus HFO and CMV through the recruitment of previously nonaerated lower lung units.

Acknowledgments This work has been funded by the Thorax Foundation, Athens, Greece.

References

- Mentzelopoulos SD, Roussos C, Koutsoukou A, Sourlas S, Malachias S, Lachana A, Zakynthinos SG (2007) Acute effects of combined high-frequency oscillation and tracheal gas insufflation in severe acute respiratory distress syndrome. *Crit Care Med* 35:1500–1508
- Dolan S, Derdak S, Solomon D, Farmer C, Johannigman J, Gelineau J, Smith RB (1996) Tracheal gas insufflation combined with high-frequency oscillatory ventilation. *Crit Care Med* 24:456–465
- Mentzelopoulos SD, Malachias S, Kokkoris S, Roussos C, Zakynthinos SG (2010) Comparison of high-frequency oscillation and tracheal gas insufflation versus standard high-frequency oscillation at two levels of tracheal pressure. *Intensive Care Med* 36:810–816
- Nahum A (1998) Equipment review: tracheal gas insufflation. *Crit Care* 2:43–47
- Slutsky AS, Berdine GG, Drazen JM (1980) Steady flow in a model of human central airways. *J Appl Physiol* 49:417–423
- Puybasset L, Cluzel P, Chao N, Slutsky AS, Coriat P, Rouby JJ, CT Scan ARDS Study Group (1998) A computed tomography scan assessment of regional lung volume in acute lung injury. *Am J Respir Crit Care Med* 158:1644–1655
- Malbuisson LM, Busch CJ, Puybasset L, Lu Q, Cluzel P, Rouby JJ, CT Scan ARDS Study Group (2000) Role of the heart in the loss of aeration characterizing lower lobes in acute respiratory distress syndrome. *Am J Respir Crit Care Med* 161:2005–2012
- Rouby JJ, Puybasset L, Nieszkowska A, Lu Q (2003) Acute respiratory distress syndrome: lessons from computed tomography of the whole lung. *Crit Care Med* 31(Suppl):S285–S295
- Gattinoni L, Caironi P, Pelosi P, Goodman LR (2001) What has computed tomography taught us about the acute respiratory distress syndrome? *Am J Respir Crit Care Med* 164:1701–1711
- Solway J, Rossing TH, Saari AF, Drazen JM (1986) Expiratory flow and dynamic pulmonary hyperinflation during high-frequency ventilation. *J Appl Physiol* 60:2071–2078
- Luecke T, Herrmann P, Kraincuk P, Pelosi P (2005) Computed tomography scan assessment of lung volume and recruitment during high-frequency oscillation. *Crit Care Med* 33(Suppl):S155–S162
- Malbuisson LM, Muller JC, Constantin JM, Lu Q, Puybasset L, Rouby JJ, CT Scan ARDS Study Group (2001) Computed tomography assessment of positive end-expiratory pressure-induced alveolar recruitment in patients with acute respiratory distress syndrome. *Am J Respir Crit Care Med* 163:1444–1450
- Gattinoni L, Caironi P, Cressoni M, Chiumello D, Ranieri VM, Quintel M, Russo S, Patroniti N, Cornejo R, Bugeo G (2006) Lung recruitment in patients with the acute respiratory distress syndrome. *N Engl J Med* 354:1775–1786
- Bernard GR, Artigas A, Brigham KL, Carlet J, Falke K, Hudson L, Lamy M, Legall JR, Morris A, Spragg R, The Consensus Committee (1994) The American-European consensus conference on ARDS. Definition, mechanisms, relevant outcomes, and clinical trial coordination. *Am J Respir Crit Care Med* 149:818–824
- Murray JF, Matthay MA, Luce JM, Flick MR (1988) An expanded definition of the adult respiratory distress syndrome. *Am Rev Respir Dis* 138:720–723
- The Acute Respiratory Distress Syndrome Network (2000) Ventilation with lower tidal volumes as compared with traditional tidal volumes for acute lung injury and the acute respiratory distress syndrome. *N Engl J Med* 342:1301–1308

17. Mentzelopoulos SD, Roussos C, Zakyntinos SG (2005) Prone position reduces lung stress and strain in severe ARDS. *Eur Respir J* 25:534–544
18. Goldman LW (2007) Principles of CT and CT technology. *J Nucl Med Technol* 35:115–128
19. Goldman LW (2008) Principles of CT: multislice CT. *J Nucl Med Technol* 36:57–68
20. Pelosi P, Goldner M, McKibben A, Adams A, Echer G, Caironi P, Lossapio S, Gattinoni L, Marini JJ (2001) Recruitment and derecruitment during acute respiratory failure. An experimental study. *Am J Respir Crit Care Med* 164:122–130
21. Crotti S, Mascheroni D, Caironi P, Pelosi P, Ronzoni G, Mondino M, Marini JJ, Gattinoni L (2001) Recruitment and derecruitment during acute respiratory failure. A clinical study. *Am J Respir Crit Care Med* 164:131–140
22. Puybasset L, Gusman P, Muller JC, Cluzel P, Coriat P, Rouby JJ, CT Scan ARDS Study Group (2000) Regional distribution of gas and tissue in acute respiratory distress syndrome. III. Consequences for the effects of positive end-expiratory pressure. *Intensive Care Med* 26:1215–1227
23. Puybasset L, Cluzel P, Gusman P, Grenier P, Preteux F, Rouby JJ, CT Scan ARDS Study Group (2000) Regional distribution of gas and tissue in acute respiratory distress syndrome. I. Consequences for lung morphology. *Intensive Care Med* 26:857–869
24. Luecke T, Meinhardt JP, Herrmann P, Weisser G, Pelosi P, Quintel M (2003) Setting mean airway pressure during high-frequency oscillatory ventilation according to the static pressure–volume curve in surfactant-deficient lung injury. A computed tomography study. *Anesthesiology* 99:1313–1322
25. Derdak S, Mehta S, Stewart TE, Smith T, Rogers M, Buchman TG, Carlin B, Lawson S, Granton J, Multicenter oscillatory ventilation for acute respiratory distress syndrome trial (MOAT) study investigators (2002) High-frequency oscillatory ventilation for acute respiratory distress syndrome in adults: a randomized, controlled trial. *Am J Respir Crit Care Med* 166:801–808
26. Frantz ID 3rd, Close RH (1985) Alveolar pressure swings during high frequency ventilation in rabbits. *Pediatr Res* 19:162–166
27. Ferguson ND, Chiche JD, Kacmarek RM, Hallett DC, Mehta S, Findlay GP, Granton JT, Slutsky AS, Stewart TE (2005) Combining high-frequency oscillatory ventilation and recruitment in adults with early acute respiratory distress syndrome: the treatment with oscillation and an open lung strategy (TOOLS) trial pilot study. *Crit Care Med* 33:479–486
28. Funk DJ, Lujan E, Moretti EW, Davies J, Young CC, Patel MB, Vaslef SN (2008) A brief report: the use of high-frequency oscillatory ventilation for severe pulmonary contusion. *J Trauma* 65:390–395
29. Gattinoni L, Carlesso E, Cadringer P, Valenza F, Vagginelli F, Chiumello D (2003) Physical and biological triggers of ventilator-induced lung injury and its prevention. *Eur Respir J* 22(Suppl 47): 15s–25s
30. Vieira SR, Nieszkowska A, Lu Q, Elman M, Sartorius A, Rouby JJ (2005) Low spatial resolution computed tomography underestimates lung overinflation resulting from positive pressure ventilation. *Crit Care Med* 33:741–749
31. Reske AW, Busse H, Amato MB, Jaekel M, Kahn T, Schwarzkopf P, Schreiter D, Gottschaldt U, Seiwerts M (2008) Image reconstruction affects computer tomographic assessment of lung hyperinflation. *Intensive Care Med* 34:2044–2053
32. Vieira SR, Puybasset L, Lu Q, Richecoeur J, Cluzel P, Coriat P, Rouby JJ (1999) A scanographic assessment of pulmonary morphology in acute lung injury. Significance of the lower inflection point detected on the lung pressure–volume curve. *Am J Respir Crit Care Med* 159:1612–1623
33. Borges JB, Okamoto VN, Matos GF, Carames MP, Arantes PR, Barros F, Souza CE, Victorino JA, Kacmarek RM, Barbas CS, Carvalho CR, Amato MB (2006) Reversibility of lung collapse and hypoxemia in early acute respiratory distress syndrome. *Am J Respir Crit Care Med* 174:268–278
34. Reske AW, Reske AP, Gast HA, Seiwerts M, Beda A, Gottschaldt U, Josten C, Schreiter D, Heller N, Wrigge H, Amato MB (2010) Extrapolation from ten sections can make CT-based quantification of lung aeration more practicable. *Intensive Care Med* 36:1836–1844
35. Malachias S, Kokkoris S, Zakyntinos S, Mentzelopoulos SD (2009) High frequency oscillation and tracheal gas insufflation for severe acute respiratory distress syndrome: results from a single-center, phase II, randomized controlled trial [NCT00416260] [abstract]. *Intensive Care Med* 35(Suppl 1):S6
36. Pillow JJ (2005) High-frequency oscillatory ventilation: mechanisms of gas exchange and lung mechanics. *Crit Care Med* 33(Suppl):S135–S141